EXHIBIT Y

TO DECLARATION OF SCOTT D. TANNER, PHD.

U.S. Patent Application Ser. No. 10/614,115

ARTICLE

Characterization of a gadolinium-tagged modular contrast agent by element and molecular mass spectrometry†

Ralf Krüger,[a] Klaus Braun,[b] Rüdiger Pipkorn[c] and Wolf D. Lehmann*[a]

[a]*Central Spectroscopy, German Cancer Research Center (DKFZ), Im Neuenheimer Feld 280, 69120 Heidelberg, Germany. E-mail: wolf.lehmann@dkfz.de; Fax: ++49-6221-424554; Tel: ++49-6221-424563*

[b]*Clinical Cooperation Unit Radiation Oncology, German Cancer Research Center (DKFZ), Heidelberg, Germany*

[c]*Central Peptide Synthesis Unit, German Cancer Research Center (DKFZ), Heidelberg, Germany*

Received 2nd December 2003, Accepted 4th February 2004
First published as an Advance Article on the web 17th March 2004

A modular gadolinium-tagged contrast agent for magnetic resonance imaging has been characterized by mass spectrometry. The synthetic construct exhibits a molecular weight of about 8 kDa and is composed of three modules, (i) a diethylene triamine pentaacetic acid (DTPA) module for complexation of Gd^{3+}, (ii) a peptide nucleic acid (PNA) sequence for hybridisation with a complementary nucleic acid sequence, and (iii) a peptide transmembrane transport module. Electrospray mass spectrometry (nanoESI-MS) was used for determination of the molecular weight of the intact functional peptide and of a synthetic intermediate. In general, signals were observed for both the Gd-complexed and uncomplexed forms. For measurement of the Gd saturation size-exclusion chromatography (SEC) was coupled on-line to high-resolution inductively coupled plasma mass spectrometry (ICP-MS) and ^{32}S, ^{34}S and ^{157}Gd were simultaneously monitored. The monitoring of sulfur as a marker element for the organic part of the molecule is possible due to the presence of a disulfide bridge and a methionine residue. The molar Gd/S ratio provides a measure of the Gd saturation, which was found to be in the range of 55% to 85% in the samples investigated. Moreover, a small amount of iron tightly complexed to the contrast agent constructs was detected and was probably taken up during synthesis or purification. Thus, the combined application of SEC-ICP-MS and nanoESI-MS delivers the complementary element and molecular information required for a reliable characterization of metal-tagged contrast agents of complex, modular design.

Introduction

The traditional focus of inductively coupled plasma ionisation mass spectrometry (ICP-MS)[1,2] is quantitative trace analysis and speciation of metals.[3,4] In metal speciation studies, a separation method is usually hyphenated to ICP-MS for the selective detection of a series of compounds which contain the metal of interest but have different molecular structures. Metals and metalloids can be linked to organic compounds *via* covalent bonds, ionic interactions or some intermediate form of binding. Thus, these compounds or complexes can exhibit a wide range of stabilities, which makes their molecular analysis a challenging task. Currently, the analysis of (semi)metals coordinated to biomolecules, in particular to peptides and proteins,[5–8] attracts increasing attention due to the physiological relevance of bioinorganic complexes. The molecular characterization of organic (macro)molecules and of intact bioinorganic complexes has considerably improved since the emergence of soft ionisation techniques such as electrospray ionisation (ESI) and matrix-assisted laser desorption/ionisation. The combined use of ESI- and ICP-MS in conjunction with liquid chromatography or capillary electrophoresis has been successfully demonstrated for the analysis of organo-metalloid compounds containing selenium[9] or arsenic.[10]

Improvements in ICP-MS have extended its applicability for the detection of non-metallic elements and enabled the characterization of biomolecules by detection of phosphorus,[11–13] sulfur,[14,15] or halogens.[16,17] *Via* these elements small biomolecules and biopolymers, such as phospholipids,[17,18] (phospho)proteins,[11–15,19] and nucleotides[20] become amenable to ICP-MS analysis. For detection of nonmetal elements that are important in the biosphere, the sensitivity of ICP-MS is not as spectacular as that observed for metals. However, the sensitivity achieved still qualifies ICP-MS as an attractive tool for the biological sciences, especially when it is combined with molecular MS techniques such as ESI.[21,22]

In current bio-applications ICP-MS is often hyphenated to miniaturized separation techniques such as capillary liquid chromatography (LC) or capillary electrophoresis (CE).[5,11,23–25] On-line coupling to a separation technique increases the tolerance for background, which in biological applications is often of substantial intensity. Moreover, the use of gentle separation techniques, in particular size-exclusion chromatography (SEC) and CE, can preserve the intact, noncovalently linked metal/biomolecule complexes occurring in metallothioneins[5,24] and metalloproteins.[25,26] A further benefit is achieved when more than one element is monitored since element ratios may provide stoichiometric information for individual analytes, as has been demonstrated for zinc/iron,[26] phosphorus/sulfur,[19,27] and metal/sulfur[25,28] in peptides and proteins.

In this report the characterization of a modular gadolinium-containing contrast agent for magnetic resonance imaging is described. SEC-ICP-MS was employed for the analysis of the stoichiometric ratio between the complexed metal and the biopolymer ligand *via* simultaneous determination of Gd and S, and the intact complex was characterized by nanoESI-MS.

Materials and methods

Synthetic procedures

Synthesis of a c-*myc*-specific DTPA-PNA complex. The synthesis of the c-*myc*-specific peptide nucleic acid (PNA) sequence

† Presented at the 4th International Conference on High Resolution Sector Field ICP-MS, Venice, Italy, October 15–17, 2003.

DOI: 10.1039/b315649d

(ATGCCCCTCAACGTTAGCTT) was performed with a peptide synthesizer model 431 A (Applied Biosystems, Foster City, CA, USA) on a 0.10 mmol scale using PNA methodology. This sequence of 20 peptide nucleic acids was incorporated into a DTPA-PNA construct with the following structure: DTPA-Lys-Lys-PNA-Cys-NH_2.

Synthesis of a membrane transport peptide. The peptide was synthesized with a fully automated synthesizer Syro II (MultiSynTech, Witten, Germany) using standard Fmoc chemistry.[29] The transmembrane peptide Thr-Gln-Val-Lys-Ile-Trp-Phe-Gln-Asn-Arg-Arg-Met-Lys-Gln-Lys-Lys-Cys-NH_2 was prepared on a Rink Amide-Novagel HL resin (Novabiochem, Bad Soden, Germany), and the following groups were chosen for protecting sidechain functionalities: *t*-butyloxycarbonyl for lysine and tryptophan; *t*-butyl for threonine; 2,2,4,6,7-pentamethyldihydrobenzofurane-5-sulfoxyl for arginine; and triphenylmethyl for glutamine, asparagine and cysteine.

Coupling of the PNA to the peptide module. The membrane transport peptide and the DTPA-PNA module were oxidatively coupled at a concentration of 2 mg ml^{-1} in a 20% DMSO 80% water solution, resulting in the formation of the mixed disulfide DTPA-PNA-S-S-peptide. The oxidation was monitored by analytical C_{18} reversed-phase HPLC and was found to be nearly complete after 5 h.

Gd^{3+}[DTPA]-complex formation. Gadolinium complexation was performed as the last step by incubation of the corresponding construct with a roughly two-fold molar excess of $GdCl_3$ (Sigma-Aldrich, Deisenhofen, Germany) in aqueous NaCl (0.9%) for 12 h.

Purification procedures. All products were precipitated in ether and purified using an LC-8A preparative HPLC system (Shimadzu, Kyoto, Japan) and an ODS-A 7A reversed-phase column (S-7 μm, 20 × 250 mm) (YMC, Schermbeck, Germany), using 0.1% aqueous TFA (A) and 60:40:0.1 (v/v/v) acetonitrile/water/TFA (B) as eluents. Peptides were eluted with a linear gradient, increasing from 25% B to 60% B in 49 min at a flow rate of 10 ml min^{-1}. The fractions containing the purified conjugate were lyophilised. Intermediate products as well as the final modular construct were characterized with an LC-10 analytical HPLC (Shimadzu Kyoto, Japan) using a Pack Pro C_{18} reversed phase column type (S-5 μm, 120 A, 150 × 4.6 mm id) (YMC, Schermbeck, Germany) with 0.1% aqueous TFA (A) and 80:20:0.1 (v/v/v) acetonitrile/water/TFA (B) as eluents. The eluent gradient ranged from 5% to 80% B in 35 min.

Analytical methods

NanoESI mass spectrometry. NanoESI mass spectra were recorded using a hybrid Q-TOF mass spectrometer (Q-TOF 2, Micromass, Manchester, UK). Spray capillaries were manufactured in-house using a P-87 micropipette puller (Sutter Instruments, Novato, CA, USA) and coated with a semitransparent film of gold in an SCD 005 sputter coater (BAL-TEC AG, Balzers, Liechtenstein). Samples were desalted using ZipTip micropipette tips packed with C_{18} reversed-phase material (Millipore, Billerica, MA, USA) and eluted with 50% acetonitrile/1% formic acid for nanoESI-MS measurements. The mass accuracy for molecular weight determinations in the range 5 to 10 kDa was found to be ±100 ppm (±3 SDs) with external calibration using 10 mM aqueous phosphoric acid.

Size-exclusion chromatography. For HPLC a dual-syringe solvent delivery system (type 140 B Applied Biosystems, Foster City, CA, USA) was used. Samples were injected using a 5 μl stainless steel sample loop. Size-exclusion LC analysis was performed on a TSKgel SuperSW3000 gel filtration column (4.6 mm id × 300 mm, 4 μm particle size, separation range 5–150 kDa) protected by a 3.5 cm TSKgel SuperSW guard column (4.6 mm id × 35 mm), both columns from Tosoh Bioscience, Stuttgart, Germany. The eluent was 170 mM aqueous sodium acetate/acetic acid (pH 4.75) at a flow rate of 150 μl min^{-1}. The separation range of the column is 5–150 kDa.

ICP-mass spectrometry. ICP mass spectra were recorded on a sector-field mass spectrometer (Element 2, Thermo Finnigan, Bremen, Germany) at medium resolution (4000). The ICP mass spectrometer was tuned and calibrated by infusion of a 5 ng ml^{-1} multielement standard solution (Merck, Darmstadt, Germany) *via* a syringe pump (type 01760, Harvard Apparatus, Holliston, MA, USA), resulting in the following instrumental settings: cool gas flow 15.5 l min^{-1}, sample and auxiliary gas flow 1.1–1.2 l min^{-1}, rf power 1210 W. A low-volume spray chamber equipped with a microflow nebulizer (type PFA 100, Elemental Scientific, Omaha, NE, USA) was used as LC-ICP-MS interface. The outlet capillary of the LC was connected directly to the nebulizer. ICP-MS sensitivity factors for Gd and S were determined by direct infusion *via* a syringe pump of aqueous standards prepared from $GdCl_3 \cdot 6\,H_2O$ and Na_2SO_4 at a molar ratio of 1:10 using the same solvent and flow rate as described for SEC-ICP-MS analysis.

Results and discussion

Structure of the synthetic contrast agent

Gadolinium complexed by a chelator, such as DTPA, is widely used as a paramagnetic contrast agent for MRI.[30] However, its current clinical application is confined to imaging of the vascular and interstitial space, since the complexes generally cannot cross cellular membranes. Transmembrane transport of a diagnostic or therapeutic probe, such as antisense PNA, has been demonstrated for PNAs linked to a somatostatin analog[31] or to a general membrane transport module. With the latter approach, MRI contrast enhancement can be extended to intracellular compartments.[32–34] For imaging of the cytosolic compartment a modular contrast agent was synthesized, comprising (i) a DTPA metal chelator, (ii) a 22 mer antisense (*anti-myc*) PNA, and (iii) a 16 mer transport peptide. A Lys-Lys bridge was used to link the DTPA and PNA modules *via* amide bonds, whereas the transport peptide and the PNA were connected by formation of a Cys-Cys disulfide bridge, as displayed schematically in Fig. 1.

The transport peptide unit acts as a non-cell-specific cytoplasmic import module[35,36] resulting in internalisation of the intact construct. The PNA part may hybridise intracellularly with complementary oligonucleotide sequences. This process is supported by gradual release of the transport peptide unit by cleavage of the Cys-Cys disulfide bridge in the reductive cytosolic environment.[33] The synthesis and characterization of such metal-containing modular contrast agents

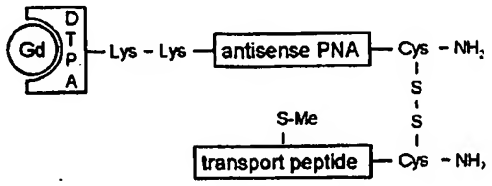

Fig. 1 Modular assembly of a synthetic paramagnetic contrast agent designed for magnetic resonance imaging (MRI) studies of gene expression. The peptide module operates as a transmembrane transporter, the PNA module hybridises to a region with complementary DNA, and the DTPA/Gd module provides T_1-weighted contrast enhancement of the intracellular ^1H MRI signal.

with MW ≈ 5–10 kDa are demanding tasks. In the following the characterization of the Gd-tagged contrast agent (see Fig. 1) and of a synthetic intermediate by molecular (ESI) and element (ICP) mass spectrometry is described.

Molecular analysis of the contrast agent by NanoESI-MS

The characterization of the modular probe as displayed in Fig. 1 involves molecular weight determination and quantitative analysis of Gd saturation. NanoESI-MS is ideally suited for molecular weight determinations due to the very soft ionisation employed, the low sample consumption and the good mass accuracy when a high resolution mass analyser is used (see Experimental section). Molecular weight measurements are best accomplished after each step of the synthetic procedure. Fig. 2 shows the nanoESI mass spectrum of the Gd-loaded synthetic intermediate [DTPA]-Lys-Lys-[PNA]-Cys-amide.

The mass spectrum in Fig. 2 indicated the presence of two compounds with average molecular weights of 6084.6 Da and 6237.6 Da. These masses are within 0.6 Da (≈ 100 ppm) of the values calculated for the elemental compositions corresponding to the synthesized product and its Gd complex ($C_{242}H_{318}N_{116}O_{75}S_1$) and ($C_{242}H_{315}N_{116}O_{75}S_1Gd$), respectively. Investigation of the shape of the two molecular ion signals provided additional support for the presence of Gd in the DTPA-PNA construct, as shown in Fig. 3.

The width or extent of the isotope pattern for the M + Gd complex (Fig. 3, top) is larger than that observed for the corresponding Gd-free product M (Fig. 3, bottom). The extension of the isotope pattern when Gd is present is due to the fact that Gd has five main isotopes with similar abundance plus two isotopes of minor abundance. Thus, the isotope pattern for Gd is superimposed on the isotope pattern of the host molecule (the sum of the patterns for C, H, N, O, and S). The monoisotopic peak for the M + Gd complex in Fig. 3 cannot be unambiguously assigned due to the low abundance (0.2%) of ^{152}Gd. In contrast, the monoisotopic peak for the Gd-free product can be readily assigned. The good agreement between the theoretical isotopic distributions (centroid pattern in Fig. 3) and the experimental isotopic patterns supports the assignments made. This analysis was further validated by determination of the isotope pattern envelopes of the M and M + Gd ion signals at half maximum (fwhm) for the charge states 4+, 5+, and 6+. The results were then converted to values corresponding to the singly charged molecule and compared with the theoretical values (Table 1).

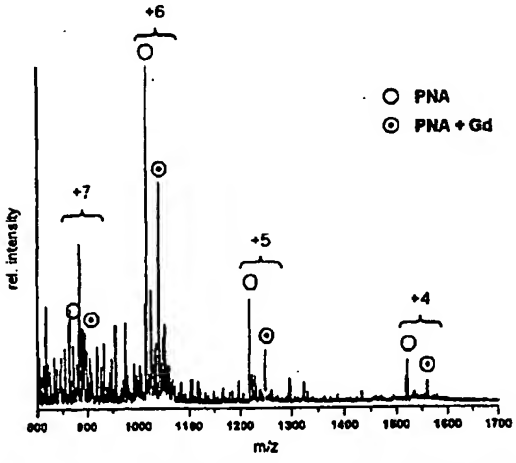

Fig. 2 Survey nanoESI mass spectrum of the gadolinium-loaded synthetic intermediate [DTPA]-Lys-Lys-[PNA]-Cys-amide of the contrast agent displayed in Fig. 1. A series of multiply charged molecular ions for Gd-free and Gd-complexed forms is observed.

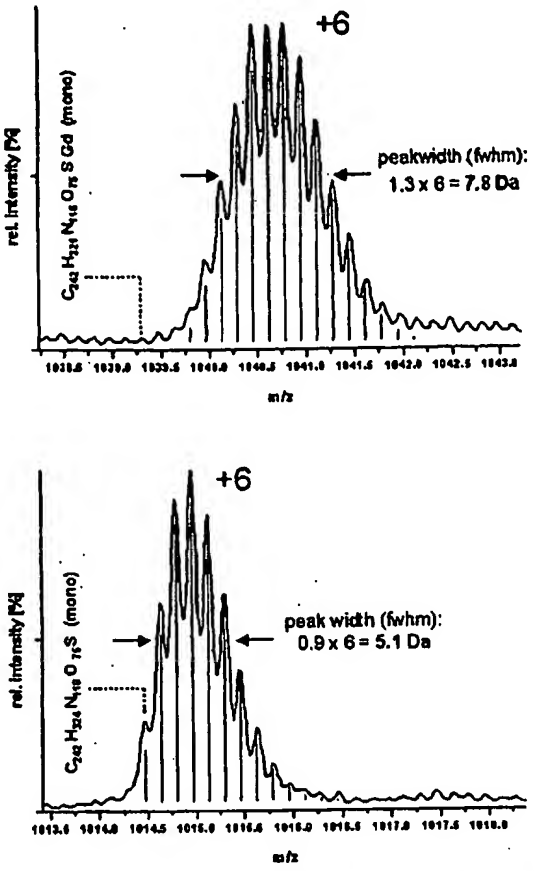

Fig. 3 Expanded display of the two molecular ion signals with charge state +6 in the nanoESI spectrum in Fig. 2. Upper trace: $[M + 3H + Gd]^{6+}$ signal; lower trace: $[M + 6H]^{6+}$ signal. The two *m/z* scales are aligned at the position of the monoisotopic signal. The underlying centroid pattern represents in each case the calculated natural isotope patterns.

The experimental isotope pattern width calculated for the M + Gd pattern exceeds that for the M pattern by 2.4 Da, which is close to the theoretical difference of +1.9 Da. Thus, the data in Table 1 are consistent with the theoretical values and provide additional, albeit indirect, evidence for the presence of the desired M + Gd complex.

Another important parameter for characterization of the contrast agent is the percent Gd saturation calculated from the ratio M + Gd/total M, which determines the amount of Gd that can be delivered into the cells. At first, one might expect

Table 1 Width of the isotope envelopes for the nanoESI molecular ion signals of the DTPA-PNA construct in free (M) and Gd-complexed (M + Gd) form. The experimental data derived from the 4+, 5+, and 6+ charge states were transformed into peak widths corresponding to the singly charged molecular ions

	Gd-free Isotope envelope width[a]/Da	Gd-complexed Isotope envelope width[a]/Da
$[M + 4H]^{6+}$	4.6	7.6
$[M + 5H]^{5+}$	5.3	6.8
$[M + 6H]^{6+}$	5.1	7.8
mean ± S.D.	5.0 ± 0.4	7.4 ± 0.5
theoretical	4.7	6.6

[a] Full width at half maximum (fwhm).

that an ESI spectrum as in Fig. 2 could be used to calculate the Gd saturation since the M + Gd species do not decompose in the solution used for ESI analysis nor during the electrospray ionisation process itself (data not shown). However, there are reasons to doubt that an ESI spectrum can give unbiased values for Gd saturation. It has been documented that the ESI response is concentration-dependent and sensitive to minor structural changes in the analytes, including complex formation.[15,37,38] Partitioning during droplet formation and solvent evaporation is widely accepted as a possible explanation. Although these effects are minimized for nanoESI compared to conventional ESI[39,40] due to the low flow rate of about 20 nl min^{-1}, the responses for the metal-complexed and the non-complexed forms of the constructs cannot be presumed to be identical. This caveat is further substantiated by the observation that M/M + Gd ion pairs with different charge states usually exhibit nonidentical intensity ratios. For these reasons ICP-MS was selected as the more suitable analytical method for quantitative determination of the Gd saturation.

Gd saturation of the contrast agent analysed by SEC-ICP-MS

The final construct as displayed in Fig. 1 contains three sulfur atoms (two in the disulfide bridge and one in the methionine residue of the transport module) and one Gd atom. The presence of a known amount of sulfur in the compounds of interest provides the basis for the quantitative determination of Gd saturation through measurement of the molar Gd/S ratio by ICP-MS. An additional analytical condition which has to be met is to separately detect complexed and free Gd^{3+} since both forms may be present in a sample of the contrast agent. Free Gd^{3+} may originate, for example, from incubation of the construct with excess Gd^{3+}, as necessary for formation of the end product, or it may originate from partial decomposition of the intact complex during storage. Therefore, LC-ICP-MS was selected to achieve this separation. The standard reversed-phase gradient system for LC-MS of peptides resulted in good separation between free and complexed Gd but induced substantial decomposition of the Gd-DTPA complex due to the low pH (0.1% TFA, pH *ca.* 1.5) of the LC eluent (data not shown). Instead, size-exclusion chromatography (SEC) at moderately acidic conditions (pH 4.75) was found to be suitable for separating the Gd-complexed constructs (mol. wt. 6–9 kDa) from free Gd^{3+} while retaining the integrity of the Gd^{3+}-DTPA complex. The SEC technique minimizes acid-catalysed release of Gd^{3+} as well as the binding of the analytes to deprotonated silanol groups of the size-exclusion column that can occur at neutral pH.

Measurement of S as $^{32}S^+$ (*m/z* 31.97207) is compromised by the occurrence of an intense isobaric $^{16}O_2^+$ signal (*m/z* 31.98983) with a separation of only 17.8 mDa. The medium resolution (4000) is sufficient to separate these ions at comparable intensities. However, the usually much larger intensity of the $^{16}O_2^+$ signal compared to that for $^{32}S^+$ means that the background level for $^{32}S^+$ detection is composed of two components: a $^{32}S^+$ component (true sulfur background) and a $^{16}O_2^+$ component (overlap from the oxygen peak). The situation becomes more favourable, as the signal of the sulfur-containing increases. Detection of sulfur as $^{34}S^+$ may represent a useful supplement to or alternative for $^{32}S^+$ detection. However, at natural abundance the intensity of the $^{34}S^+$ signal is about a factor of 25 lower than that for $^{32}S^+$. The neighbouring $^{16}O^{18}O^+$ peak is separated by only 16.2 mDa but its intensity is reduced by a factor of 250 compared to the oxygen peak at *m/z* 32. LC-ICP-MS is characterized by continuous monitoring of the background signals compared to discrete measurements in a batch procedure, thus resulting in an improved tolerance for high background levels. SEC-ICP-MS is particularly advantageous in this respect, since isocratic elution results in relatively stable background levels. Fig. 4

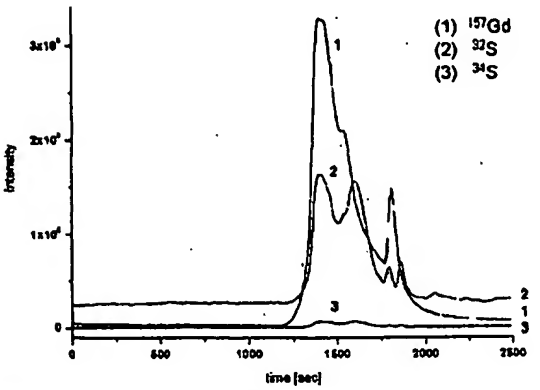

Fig. 4 SEC-ICP-MS run for *ca.* 10 nmol of the complete DTPA-PNA-peptide construct with monitoring of $^{32}S^+$, $^{34}S^+$, and $^{157}Gd^+$. The largest peak represents the Gd-complexed contrast agent. A Gd saturation of about 55% was calculated from the heights of the gadolinium and sulfur peaks. A small amount of free Gd^{3+} may result in the peak at retention time 1800 s (see Fig. 5 for comparison).

illustrates the size-exclusion chromatographic separation of the complete DTPA-PNA-peptide construct, where ^{32}S, ^{34}S and ^{157}Gd were monitored on-line by ICP-MS.

Both the ^{32}S and ^{34}S traces can be used for estimation of the Gd saturation *via* SEC-ICP-MS. For this purpose, the sensitivity factors for the two sulfur isotopes and ^{157}Gd were determined by direct infusion of standard solutions at various concentrations under the conditions used for SEC. The sensitivity factors were calculated from the calibration curves established for the corresponding isotopes ($R > 0.998$ for all isotopes). The ratios of the sensitivity factors were 12.9 for the pair $^{157}Gd/^{32}S$ and 278 for the pair $^{157}Gd/^{34}S$, respectively. The relationship between of these ratios is 0.0464, which is in good agreement with the natural $^{34}S/^{32}S$ isotopic ratio of 0.0452.[41] Using these factors and the data in Fig. 4, the Gd saturation of the contrast agent sample is calculated to be 56% based on the ^{32}S-trace and 55% based on the ^{34}S-trace.

The Gd saturation can be increased by addition of excess Gd^{3+}. Fig. 5 shows a SEC-ICP-MS run after incubation of the DTPA-PNA-Peptide contrast agent with excess $GdCl_3$ overnight and without purification before analysis. In this case the Gd saturation was determined to be 84%. It is evident from Fig. 5, that the resolving power of the size-exclusion column was sufficient to separate the Gd-complexed contrast agent from free Gd^{3+}. For the analysis shown in Fig. 5 *ca.* 80 pmol of sample were injected, *i.e.*, an amount that was *ca.* 150 times less than that injected for the analysis shown in Fig. 4. The signal-to-noise ratio for the $^{34}S^+$ trace in Fig. 5b is only about a factor of two lower than that for $^{32}S^+$ (Fig. 5a). The much lower sensitivity of $^{34}S^+$ compared to $^{32}S^+$ is compensated to a large extent by a reduction in the background at *m/z* 34.

Stability of the Gd complex and metal exchange

The final DTPA-PNA-peptide construct was also analysed by nanoESI-MS as shown in Fig. 6a.

One of the most intense signals was identified as the intact Gd-complexed contrast agent (C_{340} H_{477} N_{148} O_{98} S_3 Gd = 8458.9, calculated average m.w.; experimental value was correct within ±100 ppm). As was the case for the intermediate product, an additional signal for the uncomplexed compound was also observed (Gd-free compound: C_{340} H_{480} N_{148} O_{98} S_3 = 8304.7, calculated average m.w.). As discussed above for Fig. 3, the incorporation of Gd results in an increase in the isotope pattern width in the deconvoluted spectrum (Fig. 6a). The signals for M and M + Gd were accompanied by a single +16 Da satellite ion, which was assigned to the oxidation

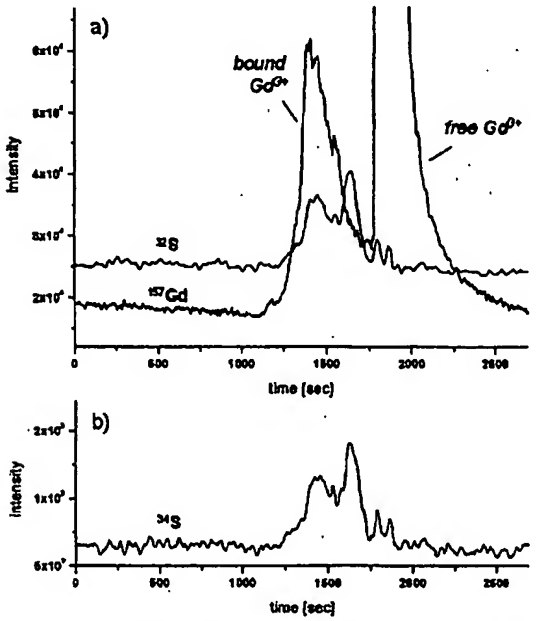

Fig. 5 SEC-ICP-MS run for *ca.* 80 pmol of the complete construct with monitoring of $^{32}S^+$, $^{34}S^+$, and $^{157}Gd^+$. Prior to analysis, the sample was incubated overnight with an excess of gadolinium chloride. (a) Traces for $^{32}S^+$ and $^{157}Gd^+$; (b) $^{34}S^+$ trace. Gd saturation of the contrast agent was calculated to be 84%. The peak representing the Gd-tagged contrast agent is followed by a large peak for free Gd^{3+}.

product carrying a methionine sulfoxide.[42] The occurrence of only a single +16 Da satellite is in agreement with the occurrence of a single methionine in the construct. The two other sulfur atoms reside in an S-S bridge which is not as readily oxidized. In the nanoESI analysis of the intermediate product (see Fig. 2) no +16 Da satellite was observed, because the methionine-containing transport peptide had not yet been attached. The assignments of the signals for M and M + Gd were further substantiated by incubation of the contrast agent with 0.1 M HCl for 1 h. As shown in Fig. 6b, this acid treatment increased the signal for M at the expense of the signal for M + Gd. The as yet unassigned group of signals for intermediate masses were more or less unaffected by this treatment.

To obtain the contrast agent in a more pure form, the raw product was subjected to SEC-ICP-MS and the first Gd-containing peak was collected and subjected to nanoESI-MS. For this purpose the excess solvent was evaporated and the lyophilised fraction was redissolved and desalted using RP-C_{18} micropipette tips. The nanoESI spectrum obtained (Fig. 6c) shows clearly that the purity of the isolated fraction has been improved (compare with Fig. 6a), particularly in the low-mass region. However, the signals for the main components appear at the positions corresponding to the unassigned signals in the raw product spectrum. The characteristic doublet (+16 Da difference) at *m/z* 8358 and at *m/z* 8374 indicates the presence of the intact contrast agent complexed with iron instead of gadolinium. The iron adduct may have formed *via* a metal-exchange reaction during lyophilisation and resolvation and the metal parts of the HPLC system may be the source of Fe^{3+}. The hypothesis of metal exchange was tested by incubating aliquots of the intact analyte with excess $FeCl_3$ or with excess $GdCl_3$, respectively. After desalting, these samples were subjected to nanoESI-MS analysis (see Fig. 7).

After incubation with Fe^{3+} (Fig. 7a), only the signal doublet corresponding to the iron adduct was detected. In the corresponding Gd^{3+}-treated sample the Gd adduct was detected as

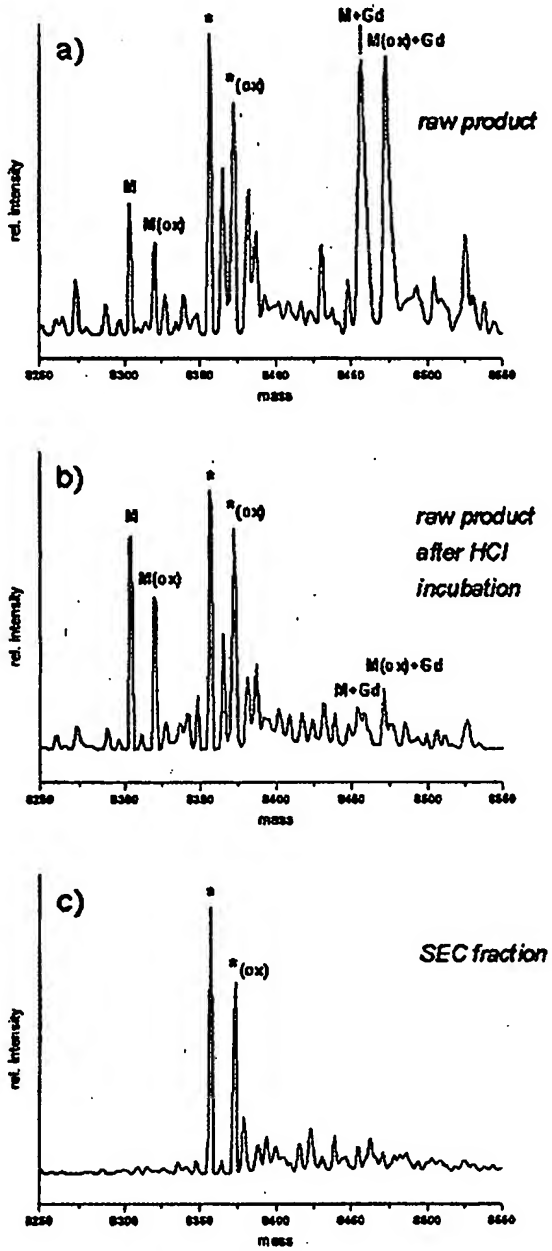

Fig. 6 Comparison of deconvoluted nanoESI spectra of the complete construct as shown in Fig. 1; (a) raw product, the most abundant signal represents the intact Gd-complexed contrast agent accompanied by a minor signal of the uncomplexed form; the ion signals marked (*) probably result from the incorporation of other metal ions; (b) raw product after incubation with 0.01 M HCl, the ion signal of the free form increased at the expense of the Gd-complexed form; (c) SEC-isolated Gd-containing fraction (see Fig. 4) after lyophilisation; it appears that in the SEC-isolated fraction the DTPA module is complexed exclusively with Fe^{3+} (marked (*), see text).

the main component with a small amount of the remaining Fe^{3+} adduct (present before incubation, see Fig. 6). Although Gd binds very strongly to the DTPA ligand ($\log K$ = 22.5[30]), the affinity of iron for DTPA is even higher ($\log K$ = 28.0[43]).

Thus, acidic conditions and the presence of undesired metal ions such as iron with high complexing capability must be avoided during synthesis since these cations may be difficult to

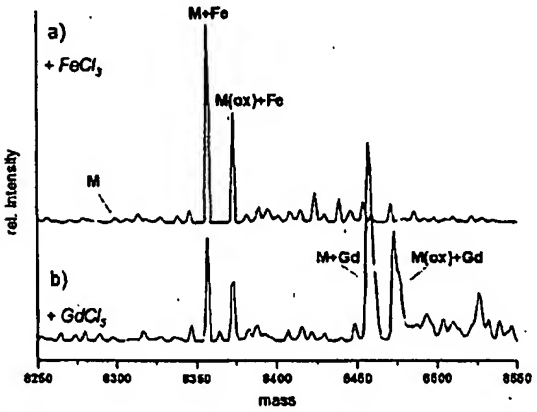

Fig. 7 Comparison of deconvoluted nanoESI signals of the purified intact contrast agent following incubation overnight with a *ca.* 10-fold molar excess of $FeCl_3$ (a) or a *ca.* 10-fold molar excess of $GdCl_3$ (b). Very little uncomplexed species can be detected after these treatments. The higher stability constant for Fe^{3+}-DTPA *vs.* Gd^{3+}-DTPA means that Gd^{3+} could not replace Fe^{3+} completely (the baseline offset between the two spectra was introduced for display purpose only).

remove once incorporated. The combined use of ICP-MS and SEC allows for a reliable determination of the Gd saturation since only moderately acidic conditions are used (pH 4.75) which have little effect on complex stability.

Conclusion

It has been shown that a complete and reliable characterization of a metal-complexed DTPA-PNA-peptide contrast agent can be achieved by the combined use of nanoESI-MS and SEC-ICP-MS with confirmation of the organic part of the complex and determination of its metal saturation level. This novel analytical strategy may be generally applicable to the characterization of metal-complexed diagnostic probes, whereby both the metal and the organic part can be separately quantified by ICP-MS. Metal-biopolymer complexes with stability constants lower than that for Gd-DTPA may also become amenable to analysis when the liquid chromatographic separation and the electrospray MS analyses can be performed at pH values closer to physiological conditions.

Acknowledgements

We are indebted to W. E. Hull for linguistic improvements and we gratefully acknowledge the support of the Bundesministerium für Bildung und Wissenschaft (Proteomics Program).

References

1 R. S. Houk, V. A. Fassel, G. D. Flesh, H. J. Svec, A. L. Gray and C. E. Taylor, *Anal. Chem.*, 1980, 52, 2283 2289.
2 *Inductively Coupled Plasma Mass Spectrometry*, ed. A. Montaser, Wiley VCH, 1998.
3 B. Michalke, *Ecotox. Environ. Safety*, 2003, 56, 122 139.
4 J. A. Caruso and M. Montes-Bayon, *Ecotox. Environ. Safety*, 2003, 56, 148 163.
5 A. Prange and D. Schaumlöffel, *Anal. Bioanal. Chem.*, 2002, 373, 441 453.
6 W. Maret, *J. Anal. At. Spectrom.*, 2004, 19, 15 19.
7 J. Szpunar, *Anal. Bioanal. Chem.*, 2003, 378, 54 56.
8 A. Sanz-Medel, M. Montes-Bayón and M. L. Fernández Sánchez, *Anal. Bioanal. Chem.*, 2003, 377, 236 247.
9 J. R. Encinar, L. Ouerdane, W. Buchmann, J. Tortajada, R. Lobinski and J. Szpunar, *Anal. Chem.*, 2003, 75, 3765 3774.
10 S. McSheehy, J. Szpunar, R. Morabito and P. Quevauviller, *Trends Anal. Chem.*, 2003, 22, 191 209.
11 M. Wind, M. Edler, N. Jakubowski, M. Linscheid, H. Wesch and W. D. Lehmann, *Anal. Chem.*, 2001, 73, 29 35.
12 D. R. Bandura, V. I. Baranov and S. D. Tanner, *Anal. Chem.*, 2002, 74, 1497 1502.
13 J. S. Becker, S. F. Boulyga, C. Pickhardt, J. Becker, S. Buddrus and M. Przybylski, *Anal. Bioanal. Chem.*, 2003, 375, 561 566.
14 E. Svantesson, J. Pettersson and K. E. Markides, *J. Anal. At. Spectrom.*, 2002, 17, 491 496.
15 M. Wind, A. Wegener, A. Eisenmenger, R. Kellner and W. D. Lehmann, *Angew. Chem. Int. Ed.*, 2003, 42, 3425 3427.
16 R. Simon, J. Tietge, B. Michalke, S. Degitz and K.-W. Schramm, *Anal. Bioanal. Chem.*, 2002, 372, 481 485.
17 B-O. Axelsson, M. Jörnten-Karlsson, P. Michelsen and F. Abou-Shakra, *Rapid Commun. Mass Spectrom.*, 2001, 15, 375 385.
18 M. Kovacevic, R. Leber, S. D. Kohlwein and W. Goessler, *J. Anal. At. Spectrom.*, 2004, 19, 80 84.
19 M. Wind, H. Wesch and W. D. Lehmann, *Anal. Chem.*, 2001, 73, 3006 3010.
20 C. Siethoff, I. Feldmann, N. Jakubowski and M. Linscheid, *J. Mass Spectrom.*, 1999, 34, 421 426.
21 V. I. Baranov, Z. A. Quinn, D. R. Bandura and S. D. Tanner, *J. Anal. At. Spectrom.*, 2002, 17, 1148 1152.
22 M. Wind and W. D. Lehmann, *J. Anal. At. Spectrom.*, 2004, 19, 20 25.
23 M. Montes-Bayon, K. DeNicola and J. A. Caruso, *J. Chromatogr., A*, 2003, 1000, 457 476.
24 R. Lobinski, H. Chassaigne and J. Szpunar, *Talanta*, 1998, 46, 271 289.
25 D. Pröfrock, P. Leonhard and A. Prange, *Anal. Bioanal. Chem.*, 2003, 377, 132 139.
26 A. Leber, B. Hemmens, B. Klösch, W. Goessler, G. Raber, B. Mayer and K. Schmidt, *J. Biol. Chem.*, 1999, 274, 37658 37664.
27 D. R. Bandura, O. I. Ornatsky and L. Liao, *J. Anal. At. Spectrom.*, 2004, 19, 96 100.
28 S. Hann, G. Koellensperger, C. Obinger, P. G. Furtmüller and G. Stingeder, *J. Anal. At. Spectrom.*, 2004, 19, 74 79.
29 A. Paquet, *Can. J. Biochem.*, 1982, 60, 976 980.
30 P. Caravan, J. J. Ellison, T. J. McMurry and R. B. Lauffer, *Chem. Rev.*, 1999, 99, 2293 2352.
31 W. Mier, R. Eritja, A. Mohammed, U. Haberkorn and M. Eisenhut, *Angew. Chem. Int. Ed.*, 2003, 42, 1968 1971.
32 S. Heckl, J. Debus, J. Jenne, R. Pipkorn, W. Waldeck, H. Spring, R. Rastert, C. W. von der Lieth and K. Braun, *Cancer Res.*, 2002, 62, 7018 7024.
33 K. Braun, P. Peschke, R. Pipkorn, S. Lampel, M. Wachsmuth, W. Waldeck, E. Friedrich and J. Debus, *J. Mol. Biol.*, 2002, 318, 237 243.
34 R. Pipkorn, W. Waldeck and K. Braun, *J. Mol. Recognit.*, 2003, 16, 240 247.
35 M. Lindgren, M. Hallbrink, A. Prochiantz and U. Langel, *Trends Pharmacol. Sci.*, 2000, 21, 99 103.
36 D. Derossi, A. H. Joliot, G. Chassaing and A. Prochiantz, *Trends Cell Biol.*, 1998, 8, 84 87.
37 P. Kebarle, *J. Mass Spectrom.*, 2000, 35, 804 817.
38 N. B. Cech and C. G. Enke, *Anal. Chem.*, 2000, 72, 2717 2723.
39 R. Juraschek, T. Dülcks and M. Karas, *J. Am. Soc. Mass Spectrom.*, 1999, 10, 300 308.
40 A. Schmidt, M. Karas and T. Dülcks, *J. Am. Soc. Mass Spectrom.*, 2003, 14, 492 500.
41 IUPAC isotope abundances 1997, http://physics.nist.gov/PhysRefData/Compositions/index.html.
42 F. M. Lagerwerf, M. vandeWeert, W. Heerma and J. Haverkamp, *Rapid Commun. Mass Spectrom.*, 1996, 15, 1905 1910.
43 N. von Wirén, S. Klair, S. Bansal, J. F. Briat, H. Khodr, T. Shiori, R. A. Kleigh and R. C. Hider, *Plant Physiol.*, 1999, 119, 1107 1114.